COLD TESTING OF RAPIDLY-CYCLING MODEL MAGNETS FOR SIS 100 AND SIS 300 – METHODS AND RESULTS*

A. Stafiniak#, C. Schroeder, E. Floch, P. Schnizer, H. Mueller, E. Fischer, G. Moritz, F. Marzouki, F. Walter, M. Kauschke, J. Kaugerts, GSI ,64291 Darmstadt, Germany

Abstract

The two synchrotrons SIS 100 and SIS 300 of the FAIR project are equipped with rapidly-cycling superconducting magnets. For quality assurance of SC magnet the Prototype Test Facility at GSI was commissioned. It allows measuring all relevant parameters of the rapidly-cycling magnets: hydraulic resistance, cryogenic losses (V-I and cryogenic method), quench behaviour and field quality.

A SIS 300 (GSI001) model dipole of the cos(θ)– type, cooled with supercritical helium, constructed at BNL, a SIS 100 superferric model dipole (4KDP6a), cooled with 2-phase helium, constructed at JINR (Dubna), were tested.

INTRODUCTION

Within an international collaboration it is planned on the GSI site to construct a new accelerator complex FAIR, which will provide high intensity primary and secondary beams of ions and antiprotons for different experiments. It will consist of 2 synchrotrons in one tunnel, SIS100 (100 Tm rigidity) and SIS300 (300 Tm rigidity), and several storage rings. The SIS100 will accelerate ions and protons at a high repetition rate and either send them to the targets for Radioactive Ion Beam (RIB) or Antiproton Beam production or to the SIS300 for further acceleration to higher energies. The Collector Ring (CR)/ Recycled Experimental Storage Ring (RESR) complex will cool the secondary beams and accumulate the antiprotons. High Energy Storage Ring (HESR) and New Experimental Storage Ring (NESR) are the experimental storage rings for antiprotons and ions, respectively [1]. Fig. 1 gives an overview of the facility.

GSI PROTOTYPE TEST FACILITY

The first planning of Prototype Test Facility (PTF) takes place in 2001. Since 2006 the test facility is in operation. The first model of SC magnet was installed and tested in September 2006. The Mandate of the PTF is:

- Test FAIR Model, Prototype and Preseries of SC magnets
- Develop Test Procedures for Factory Acceptance Tests (FAT) and Site Acceptance Tests (SAT)
- Develop Acceptance Criteria for FAT and SAT
- Develop Diagnostic Methods
- Investigate "non conforming" magnets

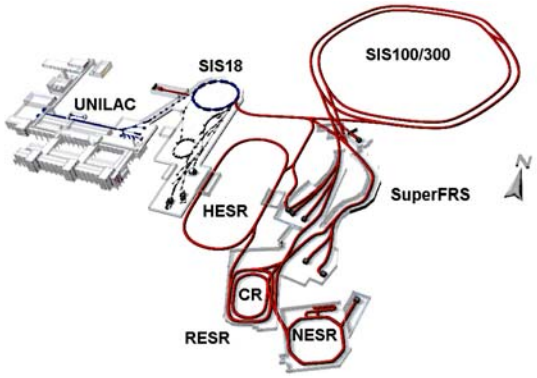

Figure 1: Overview of FAIR facility.

General Layout of Prototype Test Facility

Fig. 2. shows a schematic sketch of PTF. The PTF is equipped with a cryo-pant Linde TCF50. It has a cooling capacity of about 350W at 4.5K. The distribution box, allows using one of 3 different cooling schemes:

- bath cooling
- 2 phase flow cooling up to 5g/s
- supercritical cooling up to 200g/s

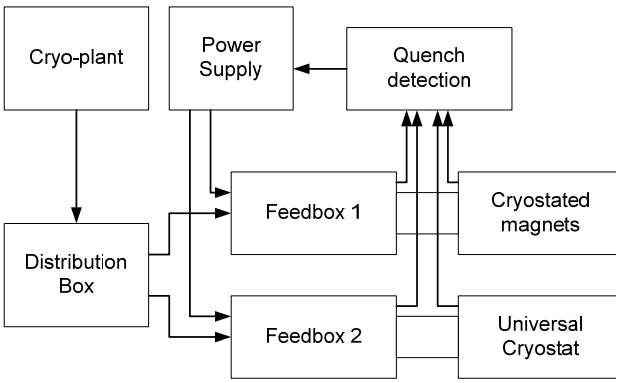

Figure 2: General layout of Prototype Test Facility.

One can vary the magnet inlet temperature down to 3.9K and the inlet pressure from 1.3bar to 5 bar. The power supply has a maximum current of 11kA (100V). The Feedboxes supply the magnets with helium and electrical current. Standard current leads (optimized for 6.5kA working up to 11kA) are made from cooper and are cooled by helium vapour.

*Work supported by EU FP6 - Design Study (contract 515873 – DIRACsecondary-Beams)
#a.stafiniak@gsi.de

The Feedboxes contains the "standard instrumentation" for:

- mass flow (warm and cold)
- temperatures
- pressures

These measured properties are used to calculate the cryogenic heat loss of a magnet.

Feedbox 1 is foreseen to test magnets with its own cryostat. At Feedbox 2 we have a universal cyostat, which allows testing only the cold mass of a magnet or other devices [2].

Quench Detection and Magnet Protection

Although most single magnets (except SIS300 dipole and quadrupole) are self-protecting, a protection system allows minimizing the recovery time (necessary for cool down) after a quench occurred due to the possibility of energy extraction. The voltage taps are isolated wires soldered to the magnet cable. Voltage differences between two symmetric coil parts of the magnet are measured. In addition an unbalanced current through a centre tap is measured. The scheme of functionality is shown in Fig.3. The main components are the separated voltage detection, the security matrix for safety actions and a data acquisition system for storage. The security matrix triggers the following safety actions:

- switch off the power converter which will switch a dump resistor into the coil circuit for energy extraction
- open the active quench valve in the feedbox
- activate the quench heaters for magnets (if applicable)

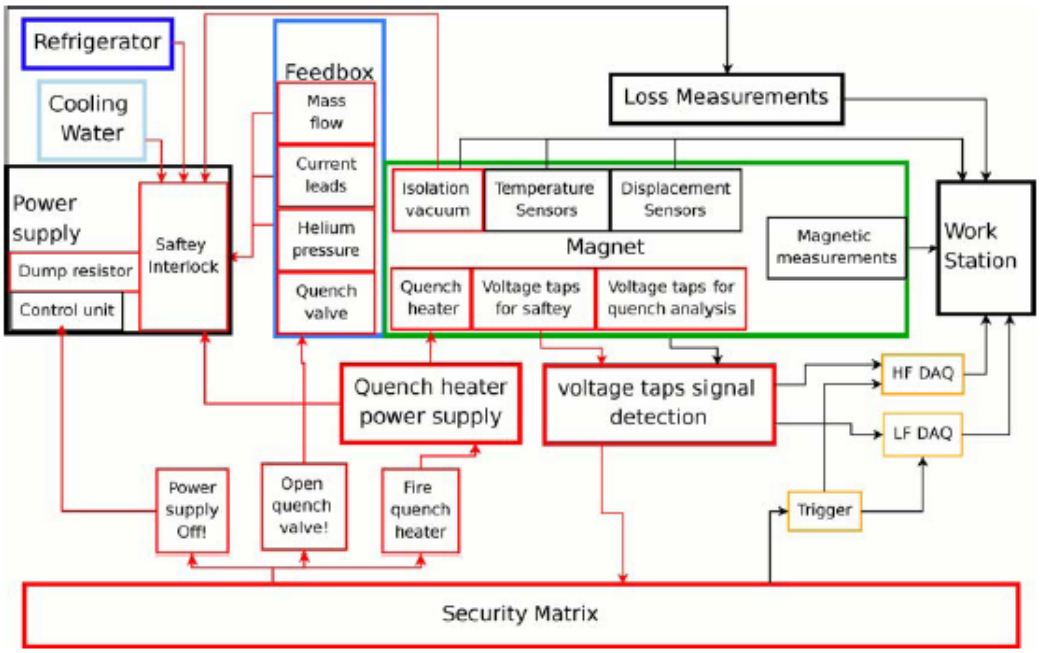

Figure 3: Scheme of the functionality of the test facility for superconducting magnets The blue parts show cooling sources. Security related devices and communication channels are given in red. Arrows show the flow of various signals. On the left the cryogenic supply, cooling water and electrical power supply are shown. The power supply provides a safety interlock, a dump resistor and its control unit. The isolation vacuum of the cryostat is monitored. The magnet is equipped with temperature sensors and displacement sensors. Voltage taps allow supervising the voltage drop on the magnet coils. Dedicated electronics treat the signal of these taps and generates triggers in case a quench has occurred (security matrix)

MEASUREMENT PRINCIPLES AND METHODS

Cryogenic losses – calorimetric method for supercritical cooling magnets (SIS300-type)

By measuring the inlet and outlet temperatures and pressures one can calculate the enthalpy difference.

The mass flow in this setup is measured directly by Coriolis sensors. Two sensors are measuring the mass flow of the current lead cooling and the mass flow at the exit of the shield at warm. One Coriolis sensor (two are shown for two different metering ranges) is measuring the total inlet mass flow at cold. Based on this measurement one can calculate the mass flow through the magnet. By knowing the magnet mass flow one can calculate the heat loss with:

$$Q_{magnet} = \dot{m}_{He} \cdot \left[h_{out}\left(T_{out}, P_{out}\right) - h_{in}\left(T_{in}, P_{in}\right) \right]$$

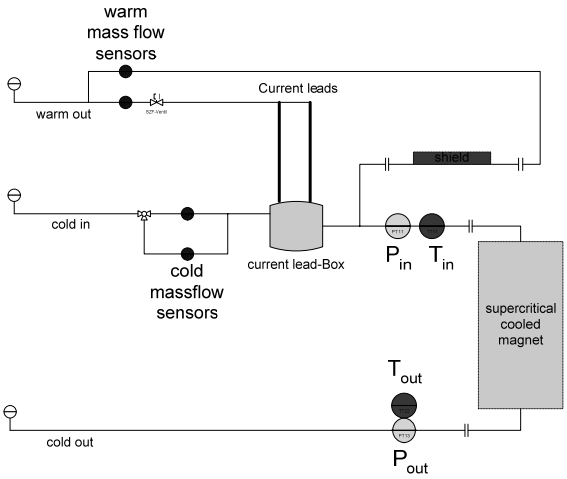

Figure 4: Cryogenic measurement of supercritical cooled magnets.

Cryogenic losses – calorimetric method for 2 phase flow cooled magnets (SIS100-type)

In this setup it's possible to measure separately the heat introduced into the coil and into the yoke. For that one varies the mass flow in order to find the mass flow at which one gets exactly 100% gas (X=1) at the coil outlet. For the coil inlet it always a pure liquid (X=0). Assuming that the total pressure drop only occurs in the coil the heat introduced is calculated by:

$$Q_{coil} = \dot{m}_{He} \cdot \left(h_{vapor}\left(x = 1, P_{out}\right) - h_{liquid}\left(x = 0, P_{in}\right) \right)$$

$$Q_{yoke} = \dot{m}_{He} \cdot \left(h_{out}\left(T_{out}, P_{out}\right) - h_{CY}\left(T_{CY}, P_{out}\right) \right)$$

The mass flow is measured by an additional overheating of the gas in the outlet line. Measuring the heater power and the temperatures before and after the heater the mass flow is given by:

$$\dot{m}_{He} = \frac{Q_{superheating}}{h_{heater\_out}\left(T_{heater\_out}, P_{out}\right) - h_{heater\_in}\left(T_{heater\_in}, P_{out}\right)}$$

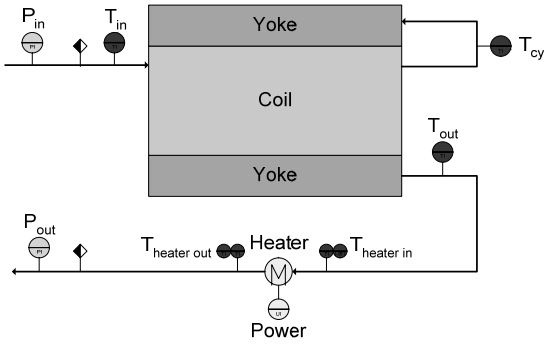

Figure 5: Cryogenic measurement of 2 phase flow cooled magnets.

Cryogenic losses – V-I method

The schematic setup of the V-I method is shown in Fig. 6. The DVM's are high accuracy digital multimeters HP 3458 A.

The current (Current DVM) is measured as indicated by the output voltage of a Zero-Flux Current Transformer (DCCT). The voltage (Voltage DVM) is measured across the magnet. The output trigger signal from Current DVM is used to trigger the Voltage DVM. The integration time of the DVMs is 20ms and the processing time (delay) between the measurements is 50µs. The power loss is calculated as the sum of the products of current and voltage over the current cycle.

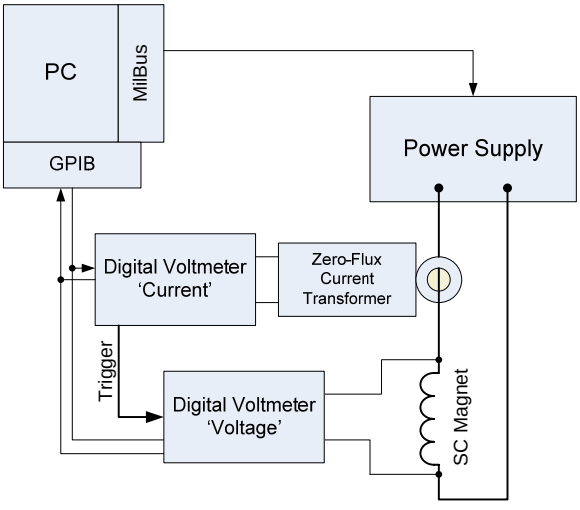

Figure 6: Set-up for losses measurement - V-I method.

The energy loss is calculated by:

$$E = \sum_{i=1}^{N} V_i \cdot I_i \cdot \Delta t_i$$

The power loss is calculated by:

$$P = \frac{1}{\sum_{i=1}^{N} \Delta t_i} E$$

with : Δti = 20.05ms , N – corresponds to 1 current cycle.

This method has several limitations. The most important are: voltage offset, measurement accuracy, measurement resolution and DVM triggering [3].

Cold Magnetic Measurements

Cold magnetic measurements are performed with the magnet at operating (cryogenic) temperatures while the measuring equipment is working at room temperature. Anti-cryostats are inserted in the magnets, wherein the measurement equipment is placed. A non-metallic anti-cryostat was fabricated to avoid additional eddy current losses in fast-ramped magnets, which can significantly distort the magnetic field quality and thus its measurement [4, 5, 6].

A "Mole" based approach was selected for measuring the superconducting magnets. A mole is a rotating coil probe based magnetometer, where the main auxiliary components (the motor, the inclinometer and the angular encoder) form an entity able to operate in high magnetic field [6].

TESTS RESULTS OF SUPERCONDUCTING MAGNETS

GSI001

GSI001 has the same coil cross section than RHIC magnets with 32 turns and 4 blocks. A phenolic spacer is placed between the coil and the iron yoke of the RHIC magnets whereas for GSI001 the coil is hold by stainless steel collars. For loss reduction a stainless steel core was inserted into the RHIC cable and the wire twist pitch was reduced. The Parameters of the GSI001 dipole are given in Table 1; a cross section of the magnet is shown in Fig. 7. The training curve of GSI001 is presented in [2].

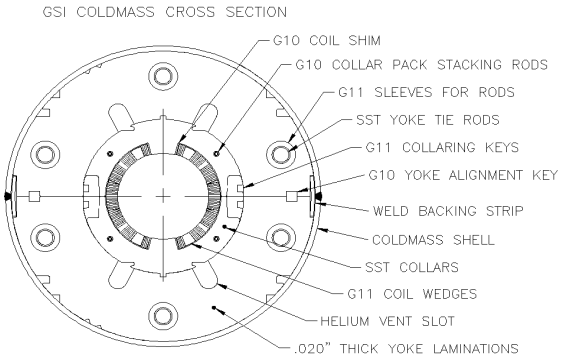

Figure 7: Cross section of GSI001 dipole

Table 1: Characteristics of the GSI001 dipole

GSI 001 characteristics	
magnet length (m)	1
I (A)	6000
Bcentral (T)	3.5
coil bore diameter (mm)	80
number of blocks	4
number of turns per pole	32
between coil and iron yoke	stainless steel collar
measured inductance (mH)	2.8
rl293K (mΩ/m)	2.551
R_2_poles_293K (Ohm)	0.394
cable length = R_2_poles_293K/ rl293K (m)	154.51
Bmax on cable / Bcentral (computed by BNL)	1.22
number of strands	30
core	2 stainless strips of 25 μm thickness each
strand diameter (mm)	0.641
α	2.21
twist pitch (mm)	4
filament diameter (μm)	6
RRR	187
R_a (μΩ)	64
R_c (mΩ)	62.5
ρ_{et} (Ωm)	1.24×10^{-10} + 0.9×10^{-10} B(T)

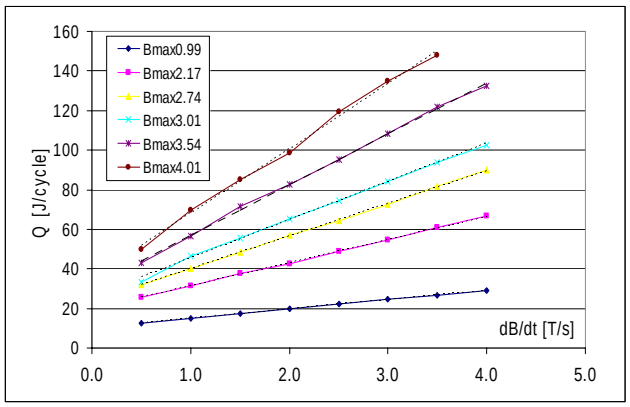

Figure 8: AC losses of GSI001 V-I method (with beam pipe), measured at GSI.

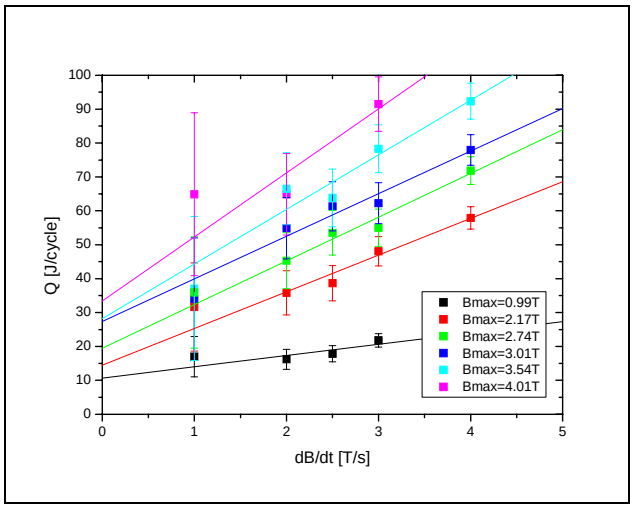

Figure 9: AC losses of GSI001 calorimetric method (with beam pipe taken at GSI).

Loss measurements have been performed electrically by BNL [7, 8] and GSI and calorimetrically by GSI alone. The results of the measurements at GSI are shown in Fig. 8 and Fig. 9 for the electrical and calorimetric methods, respectively. The results of the measurements can be split in a hysteresis part, originating from the iron hysteresis and the persistent currents in the superconductor, and an eddy current part, originating from interstrand and interfilament coupling currents in the superconductor, as well as eddy currents created in the beam tube. The contribution of the eddy currents and the hysteresis are presented in Fig. 10 and Fig 11. Calculations of the losses were performed assuming that the heat load depends linearly on the ramp rate [9]. A good agreement was found between theory and all the measurements for the hysteresis part. Concerning the eddy currents the theoretical calculations agree well with the calorimetric measurements. For the electrical measurements an enhancement of the losses can be found for magnetic fields higher than 2T. As magnetic flux leaks out from the yoke for field levels above this level, this can be explained by the presence of a thermal shield made of Cu in the cryostat used at GSI, as eddy currents are then induced into it.

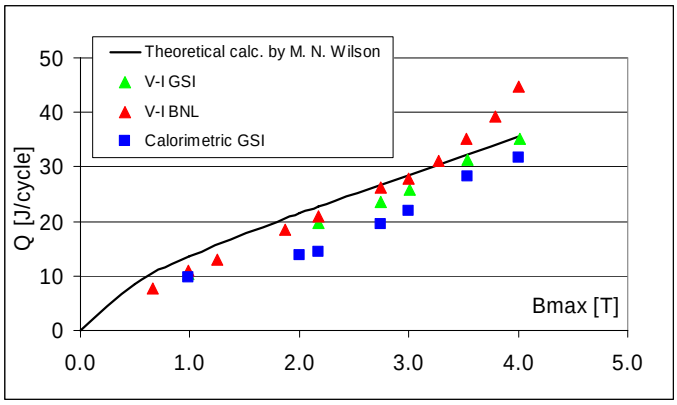

Figure 10: Hysteresis losses of GSI001 (with beam pipe)

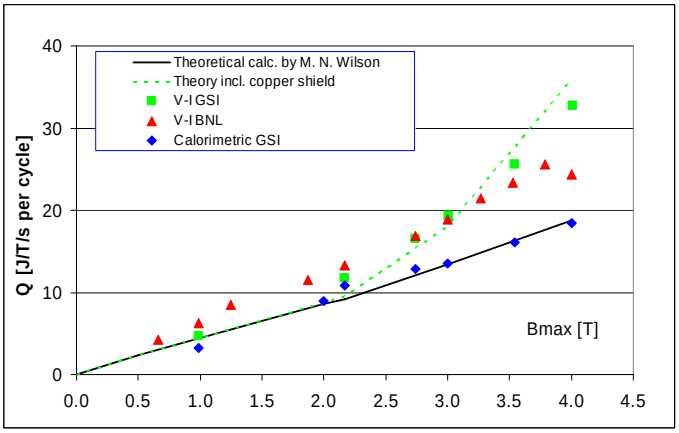

Figure 11: Eddy current losses of GSI001 (with beam pipe).

V-I loss measurements were also performed for the upper and lower half coil itself. The eddy current part of these measurements is shown in Fig. 12 together with fitting lines using the adjacent interstrand resistance Ra as a free parameter. The results seem to indicate a top-bottom asymmetry of the magnet, but this still needs further investigation.

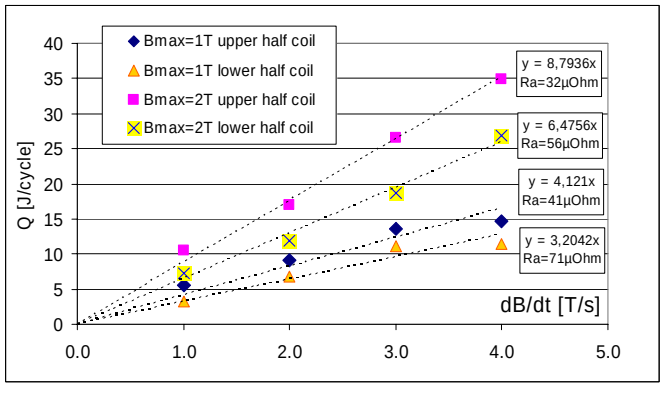

Figure 12: Top-down asymmetry of GSI 001 coil.

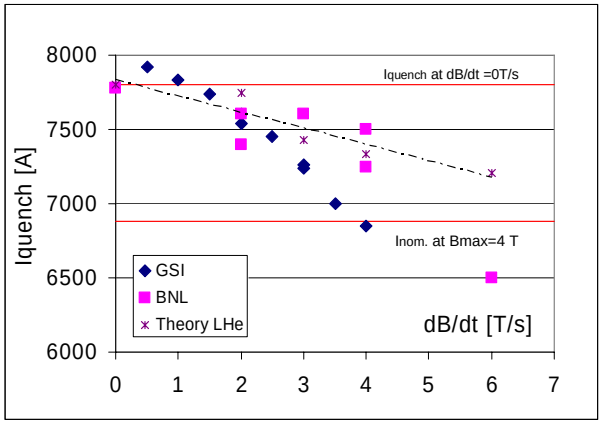

Figure 13: GSI 001 Ramp Rate Limitation. The upper red line gives the value of the DC quench current the lower red line represents the nominal operating current of the magnet.

Fig. 13 shows the measured quench current I_q as a function of the ramp rate dB/dt. The measurements at GSI were carried out in supercritical helium whereas BNL used a helium bath. As expected the cooling is more effective in the case of liquid helium. The observed curves show that the ramp rate limitation is due to AC-heating of the conductor [8, 9]

4KDP6a

The first SIS100 dipole prototype (called 4KDP6a), was tested at GSI. This magnet was manufactured in Dubna and is an upgraded version of Nuclotron magnets.

Fig. 14 presents the cable used in 4KDP6a. It is made of a CuNi tube in which the He flows and around which 31 strands (0.5 mm in diameter) are wound. One NiCr wire is used to fix the strands around the tube. The insulation is made of polyimide and impregnated fibre glass. The strand average copper ratio is 1.24 with and a RRR of 196.

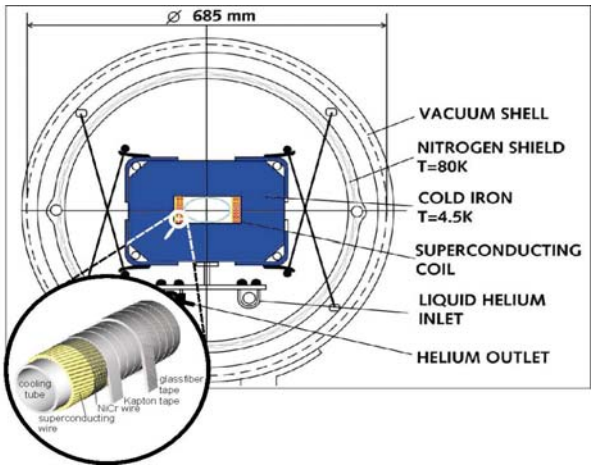

Figure 14: Cross section of 4KDP6a dipole.

Figure 15: 4KDP6a dipole (connection side).

Table 1: Characteristics of 4KDP6a dipole

4KDP6a characteristics	
iron+end plates length (m)	1.37
I (A)	5936
Bgap (T)	2
Bmax (T)	2.11
yoke gap size (mm*mm)	h=146* v=56.4
number of turns per pole	8
coil length (m)	1.475
measured inductance (mH)	1
number of strands	31
strand diameter (mm)	0.5
α	1.24
filament diameter (μm)	6
RRR	196
Tcs - 4.7 K (K)	1.53

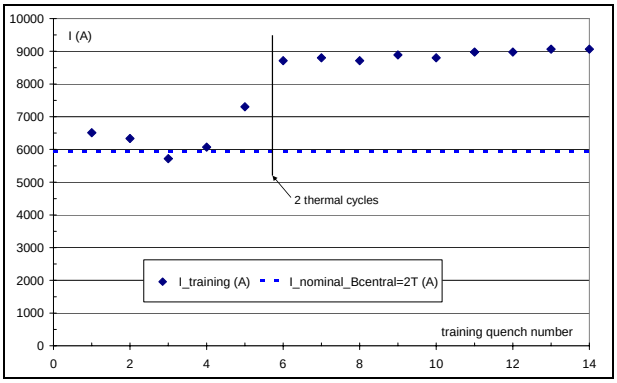

Figure 16: Training of 4KDP6a dipole (2 thermal cycles).

Fig. 16 presents the magnet training that was done in 2 steps separated by a thermal cycle. A more detailed analysis will be presented at ASC 2008 [10]

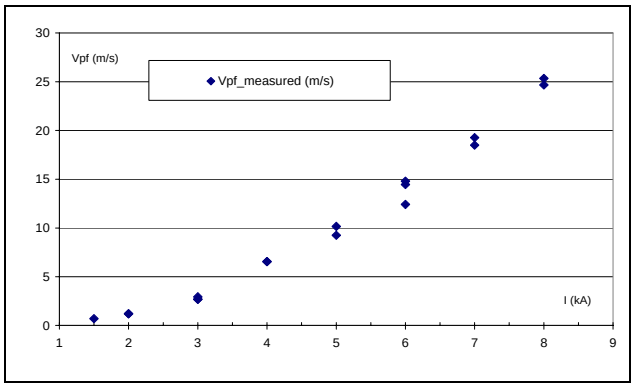

Figure 17: Quench propagation velocity in the 4KDP6a bus bars.

Because the coil is wrapped with impregnated fibre glass, it is very difficult to insert a spot heater inside the coil to investigate its quench behaviour. The quench study was therefore performed on the bus bars placed on top of the iron core.

Fig. 17 shows that the propagation velocities, measured between 1.5 and 8 kA, range from 0.7 to 25.3 m/s.

All the computations and analysis of the quench measurements performed on this magnet will be presented at ASC2008 [11].

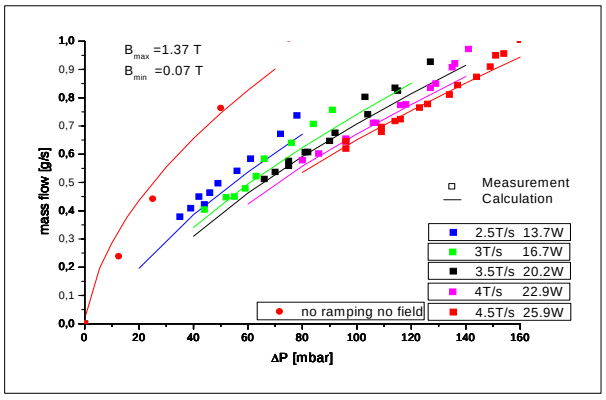

Figure 18: 4KDP6a – mass flow vs. pressure drop (2-phase flow).

Save operation of 2 phase cooled magnets requires a thorough understanding of the hydraulic behaviour and its limits. Previous studies are reported in [12] and showed that a curved single layer dipole can provide the cooling power required with the required safety margin.

As different ramp rates created different eddy current and hysteresis losses, the pressure drop of the model 4kDP6a was studied for different ramp rates and different mass flow rates and compared to calculations (see Fig. 18). The accordance allows predicting also the expected pressure drop of longer magnets as well as the mass flow rates; limited by the measurement precision as well as the required extrapolation.

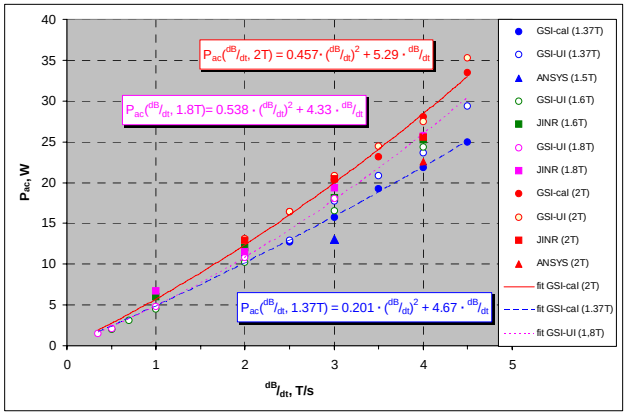

Figure 19: 4KDP6a – Calculated and measured AC Losses @ 4 K. for different ramp rates and different maximum field.

The heating power created by the eddy currents and the hysteresis was calculated using ANSYS [12, 13] and measured at JINR and at GSI (see Fig 19). One can see that the two measurement campaigns agree well and that the calculations correctly predict the magnets behaviour. Further one can clearly see that the dissipated power depends nonlinearly on the ramp rate (red curve).

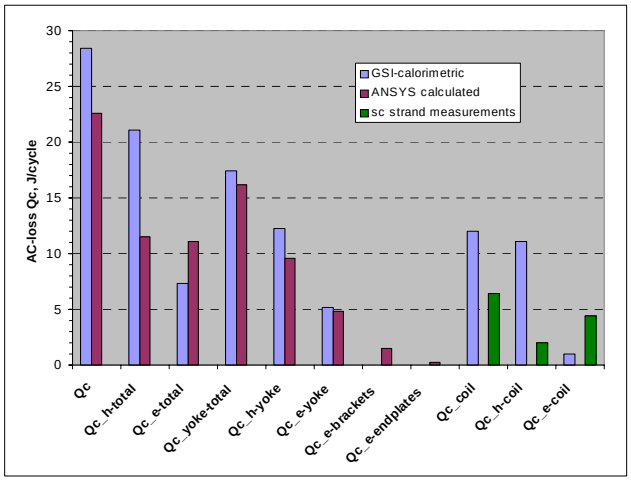

Figure 20: The heat created by the yoke and the coil. Comparison of the calorimetric measurement to the calculated data and a separate strands measurement.
Qc – total heat, Qc_h-total – total hysteresis loss,
Qy_e-total – total eddy current loss,
Qc_h-yoke – hysteresis loss in the yoke,
Qc_e-yoke – eddy current loss in the yoke,
Qc_e-brackets – eddy current loss in the brackets of magnets,
Qc_e-endplates – eddy current loss in the end-plates of magnets,
Qc_coil – the total loss in the coil,
Qc_h-coil – the hysteresis loss in the coil,
Qc_e-coil – the eddy current loss in the coil.

The calorimetric method allows separating the source of the heat impact (see Fig. 20). Further the eddy current contribution was separated by the hysteresis contribution assuming that the hysteresis contribution can be obtained extrapolating the fit curves of Fig 19 to a ramp rate of 0.

If one subtracts the strand measurements of the coil from the total heat impact measured, the measurement agrees well with the calculations. This is appropriate as the heat impact created in the coil were neglected in the model.

One can see that the larger part of the heat is created in the yoke and that the hysteresis effects are greater than the eddy current effects. The agreement is a bit worse for the subparts of the magnet. On the other hand the yoke and the coil are in thermal contact and the cooling of the yoke by the coil was not asserted separately. Thus the difference between calculation and measurement can be attributed to this unavoidable shortcoming of the experiment. All details of the magnet as well as the parameters of the materials used have to be taken into account to get numerical results matching the measurements [13].

REFERENCES

[1] FAIR – Technical Design Reports 2008

[2] A. Stafiniak, E. Floch, P. Hahne, G. Hess, M. Kauschke, F. Klos, F. Marzouki, G. Moritz, H. Mueller, M. Rebscher, P. Schnizer, C. Schroeder, G. Walter, F. Walter, H. Welker, “Commissioning of the Prototype Test Facility for Rapidly-Cycling Superconducting Magnets for FAIR”, ASC2007, August 27-31, 2007, Philadelphia, PA, USA, IEEE Trans. Appl. Superconductivity, June 2008 Volume 18, No 2, pages 1625-1628.

[3] A. Stafiniak, D. Kosobudzki, “Metrological analysis of AC losses measurement utilizing V-I method”. accepted for ASC2008.

[4] P. Schnizer et al. "Magnetic Field Characteristics of a SIS 100 Full Size Dipole", Presented at 12th European Particle Accelerator Conference, Genova 2008

[5] P. Schnizer et. al. "Superferric rapidly cycling magnets: Optimized Field Design and measurement", this publication

[6] P. Schnizer et. al. "A mole for measuring pulsed superconducting Magnets", IEEE Trans. Appl. Supercon. 18, 2008, pp 1648-1651

[7] M. N. Wilson et al, “Measured and Calculated Losses in Model Dipole for GSI´s Heavy Ion Synchrotron”, IEEE Trans. Appl. Supercon, 14,2, 2004 pp. 306-309.

[8] G. Moritz et al, “Recent Test Results of the Fast-Pulsed 4 T Cosθ Dipole GSI 001”, Proceedings of the Particle Accelerator Conference, 2005, pp.683-685

[9] M. N. Wilson et al, “Cored Rutherford Cables for the GSI Fast Ramping Synchrotron”, IEEE Trans. Appl. Supercon., 13,2, 2003, pp.1704-1709

[10] A. Stafiniak, C. Schroeder, E. Floch, F. Marzouki, F. Walter, “The GSI cryogenic test facility - measurement equipment and first experience gained on superconducting prototype magnets of the FAIR project”. Accepted for ASC2008.

[11] E.Floch, A. Stafiniak, F. Marzouki, F. Walter, C. Schroeder, H. Mueller, H. Leibrock, E. Fischer, G. Moritz, “Quench study of first SIS100 dipole prototype”. Accepted for ASC2008.

[12] E. Fischer, H. G. Khodzhibagiyan, A. D. Kovalenko, Full Size Model Magnets for the FAIR SIS 100 Synchrotron" IEEE Trans. on Appl. Supercon., 18, 2008 pp. 260-263

[13] E.Fischer, R. Kurnishov, and P. Shcherbakov, "Finite element calculations on detailed 3D models for the superferric main magnets of the FAIR SIS100 synchrotron", Cryogenics, 47, 583--594, 2007.